International Journal of Fluid Power, 2014
Vol. 15, No. 2, 69–76, http://dx.doi.org/10.1080/14399776.2014.931131

Taylor & Francis
Taylor & Francis Group

Robust Design of Piston Assemblies in an Axial Piston Pump

Shu Wang*

Eaton Corporation, Vernon Hills, Illinois, USA

The piston slipper in an axial piston pump demonstrates most complicated dynamic motions: two rotations (tilting toward to the swash plate and rotating about the pump shaft) and one translation together with the pumping piston. In addition, the slipper is used to lubricate the swash plate surface with hydraulic oil, but prevents high pressure fluid escaping from the piston bores. In hydraulic engineering, improper designs of the piston and slipper assembly cause many instability and unbalance issues while the slipper attempts to lift and tilt off the swash plate. This may cause catastrophic failure and damage to a piston pump. To suppress the undesirable motion is one of most design difficulties that might take a range of different dynamics into consideration and compromise the design parameters of piston assemblies.

In this study, the complicated dynamics are simplified and linearized with some assumptions that are able to apply stability conditions. The dynamic response of the assembly as operating needs to follow its desired rotating movement, i.e. the swash plate angular position. The slipper motion is affected by its inputs (including piston bore pressure, hold-down forces, etc.). This paper investigates the dynamic behavior of the piston and slipper assembly by using the parameter perturbation analysis (PPA) method. The results can be used as robust design recommendations for piston assemblies in the piston pump from a novel perspective.

Keywords: robust design, instability, parameter perturbation analysis, piston assembly

1. Introduction

Robust engineering design systematically analyzes the effects of variations, and makes products less sensitive to parameter variations, as well as ensuring the robust design study is completed as soon as possible within the concept start and the design release phase. The product is permitted to tolerate the given presence of variations in design and manufacturing parameters with robust design processes. For instance, in Lin and Yak (2000), the robust design is used to minimize the variation effects on micron-level alignment of optical components in the laser pickup of a compact disc system, so that the product is robust against parameter variations instead of removing variations. Alyaqout et al. (2010) combine robust design with robust control and investigate the relationship between them with an electric DC motor. To reduce the computational cost and solve the minimax control optimization problem, sequential and iterative strategies are proposed and compared to an all-in-one (Aio) strategy to address the minimax problem.

Hydraulic control systems are found in many industrial, mobile, and airborne applications and offer many distinct advantages, such as high horsepower to weight ratio, hydraulic fluid lubricating, high stiffness, and simple strategies to apply the open and closed loop control, etc. However, the design and performance analysis of hydraulic systems is complexi and difficult due to enormous nonlinearities, including fluid compressibility, laminar or turbulent flow, passage geometry, friction factors, and discharge coefficients (Merritt, 1967). In hydraulic design engineering, the approach of parameter perturbation analysis (PPA) is commonly used to adjust design factors to deal with the problem (such as stability, noise, efficiency, response speed, accuracy, etc.) and achieve a robust and optimal design. The process of the PPA is to find out what the best configuration of contributing factors is to achieve the best performance, and what the most important work is in the design.

In axial piston pumps, there is one piston cylinder combination, i.e. rotating group including a number of piston assemblies (the piston and slipper), cylinder barrel, hold-down devices, etc. Piston assemblies rotate about the drive shaft to generate the reciprocating motions with the swash plate angle, which draw fluid into each piston bore and then expel it to produce pumping flow. In the variable displacement design, the swash plate is placed at different angles to cause the pistons to move back and forth for different traveling distances in the cylinder barrel when slipper pads tilt against the swash plate surface. Three movements (reciprocating, rotating about the shaft, and tilting toward the swash plate) imply that the piston assembly is the component that presents the most complex dynamics and design difficulties in piston pumps. The piston slipper also works as a device to lubricate the swash plate surface and prevent high pressure fluid escaping from the piston bore. Therefore, if the slipper has an obvious lifting or discrepancy between its tilting angle and the swash angle, piston assemblies may be destabilized and

*Email: shw750@mail.usask.ca

cause catastrophic failure, such as slipper rolling and scoring, piston cocking and scratching, swash plate surface damaging, etc.

Much attentions has been paid to high speed translation and rotation dynamics of the slipper in previous research. To design the hydrostatic balance of a slipper, the retainer, balance pressure of no-sealing land grooves on the slipper commonly exist in the industrial designs and are used to relieve most part of hydrostatic load, up to 85% and 95%. The remaining mechanical force – about 10% – between slipper and swash plate is needed to cover hydrodynamic forces and forces of inertia. In order to examine the stability of the piston slipper, Harris et al. (1996) developed a dynamic model to predict the slipper-pads that allow lift and tilt behavior, including the effects of possible contact with the swash plate or slipper retaining plate. The oil-film parameters, slipper tilting angle, and mean clearance of the piston assembly are considered by theoretical analysis and experiments to investigate the dynamic characteristics of the slipper bearing (Iboshi and Yamaguchi, 1982, 1983). The flow rate and load carrying capacity of the slipper bearing have been investigated in theoretical and experimental methods under different deformation conditions (Manring, Johnson, et al., 2002; Manring, Wray, et al., 2004). To stabilize the motion of pistons, Yamaguchi (1976) used a type of piston with which the film thickness between the cylinder and the piston varies exponentially with respect to the longitudinal position of the piston.

Meanwhile, many researchers have addressed the pump dynamics combined with piston assemblies. The containment forces and torques on the swash plate exerted by piston assemblies have been extensively studied in Zeiger and Akers (1985) and Manring (1999, 2001). Some dynamic and steady-state models for the piston pump have been proposed and developed in the research (Schoenau, 1990; Manring and Johnson, 1996; Zhang et al., 2001). In Manring (2002), the impact of the secondary swash-plate angle is analyzed to obtain an optimal control and containment of the swash plate. A revised shape of a valve plate is proposed to improve the stability of the cylinder block dynamics and the volumetric efficiency of the pump based on numerical simulations in Ahn et al. (2005). In the study by Du (2002), the robust stability of the variable displacement piston pump can be obtained by a rugged E/H control design for the load sensing.

In this work, the dynamics of the piston and slipper assembly in a variable displacement piston pump is reviewed and analyzed. A linearized model is developed to demonstrate the dynamic characteristics of piston assemblies. Some important design parameters can be investigated by the PPA approach to consider the instability and robust design of piston assemblies. Following this introduction and literature review, mechanical dynamics and the dynamical model are derived in Section 2. Section 3 presents the main results and discussions. Concluding remarks are provided in Section 4.

2. Mechanical analyses

The schematic of a typical axial piston pump is shown in Figure 1. The inlet and outlet fluid of the pump passes through the instantaneous flow passages between the cylinder barrel and valve plate when piston assemblies are located at different angular positions. For the purpose of cost reduction, an offset between the swash rotating center and shaft axis of the pump is designed to simplify control mechanisms (i.e., removal of the bias piston). The offset is labeled as e in Figure 1. The variation between the slipper pivot center and swash rotating center is indicated as a. The swash angle α_0 is the variable that determines the pump displacement or the amount of fluid outputs per shaft revolution. In Figure 1, two coordinate systems are used to illustrate the free body diagrams of the swash plate and rotating group. The coordinate system of $x-y-z$ is used to describe the motion of the swash plate. The origin of the $x-y-z$ is located at the swash rotating center, and the $x'-y'-z'$ has the origin in the shaft axis.

Figure 2 shows the free body diagram of a piston assembly. The origin of the coordinate system $x''-y''-z''$ is defined at the gravity center of the slipper. The identical and opposite reaction force by the swash plate against the slipper is R_n. Since the tilting movement of the slipper is the main interest to study the stability condition in the research, the friction between the swash plate and slipper surfaces are not included in this case. R_n is one major force to rotate the slipper about the y''. and its exerting position is located in the

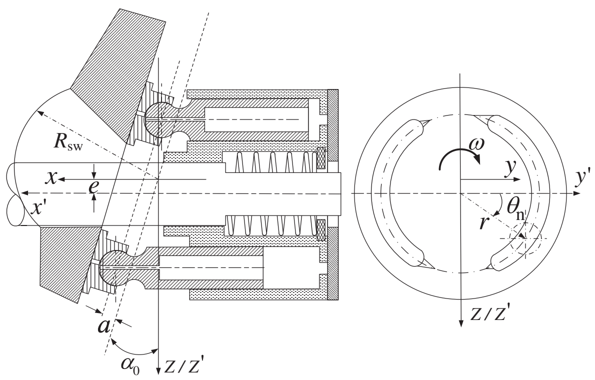

Figure 1. The schematic of an axis piston pump.

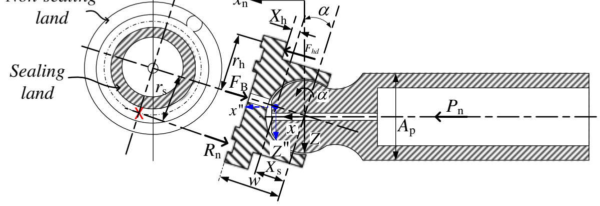

Figure 2. The free body diagram of a piston assembly.

plane of $x'' - z''$. The contact point between the swash plate and slipper can be assumed to sit on the position of average radius (that can be called as supporting radius) of sealing and nonsealing lands of slipper to prevent the excessive leakage from the piston bore to pump housing. There, the radius of the supporting radius r_s can be considered as the moment arm of R_n that makes the angular rotation about the slipper gravity center. As pumping, the slipper needs to maintain tilting position α and speed $\dot{\alpha}$ same as the swash angle α_0 and velocity $\dot{\alpha}_0$ that are desired. Otherwise, the inappropriate angles may cause the slipper pad to lift and tilt off the swash plate surface causing undesired leakage, instabilities, and even damage. In practice, the slipper is allowed to have some degree of tilting and rotating in other directions during operation. Also, the degree of tilting is an important factor that can cause a large amount of leakage, unstable flow, and even a failure of the entire pump if the tilting or rotating angle is excessive. In this study, the scale can be considered as the steady-state error range in the stability condition. All of this type of vibrating movements may be limited to a small range.

As the slipper rotates about y'', the total moment can be written (Greenwood, 1988):

$$M^{y}_{hd} + M^{y}_{Sn} + M^{y}_{n} + M^{y}_{B} - I''_{yy}\ddot{\alpha} = 0 \tag{1}$$

The moment M^{y}_{Pn} is generated by the piston pressure that can be calculated as:

$$M^{y}_{Pn} = -P_n A_P X_S \sin(\alpha) \tag{2}$$

The load point of F_{hd} is assumed to be located at the plane of $x'' - z''$ because the most interest in the study is the angular movement of the slipper about y''. Thus, the moments by the hold-down mechanism and swash plate may be written as:

$$M^{y}_{hd} = F_{hd} r_h \tag{3}$$

$$M^{y}_{n} = R_n r_s \tag{4}$$

where the moment arm of F_{hd} is determined by the radius $r_h$of the slipper retainer, and the supporting radius is r_s.

The pressure balance force F_B is generated by the pressure of the fluid film between the slipper pad and swash plate surface. The pressure balance force is a significant to enable both the slipper and piston to generate sufficient force and friction on the swash plate surface as well as to generate an oil film between the slipper and piston and the slipper and swash plate. If the sealing and nonsealing lands of slipper are designed symmetrically, back pressure flow can go through the grooves, and the deformations of slipper are not considered, the exerting point of pressure balance force will pass the piston bore center in most operating conditions. If the oil film is not designed or distributed symmetrically on the rear of slippers, the small orifice through the piston, slipper and its sealing grooves might be considered for the stability analysis.

From Manring, Johnson, et al. (2002) and Manring, Wray, et al. (2004), the balance force can be described as a linear function of piston pressure such that:

$$F_B = \xi \cdot P_n \tag{5}$$

where ξ is the coefficient that is affected by the sealing land and deformations of the slipper. However, the influence of stability analysis is not considered in this case, as F_B passes through the centerline of the slipper and results in a zero moment about y''.

Substituting Eqs. 2–4 into Eq. 1 yields:

$$-P_n A_P X_S \sin(\alpha) = F_{hd} r_h + R_n r_s - I''_{yy}\ddot{\alpha} = 0 \tag{6}$$

In the axial piston pump, the mechanical hold-down device generates a constraint force F_{hd} to slippers. F_{hd} and R_n counterbalance each other to parallel the slipper pads to the swash plate surface as shown in Figure 2. Since the piston and slipper rotate each other with a ball joint, the piston assembly can be regarded as a rigid body system. By using D'Alembert's principle, the total forces exerting on the assembly along x and z can be written as:

$$A_P P_n - (F_B + R_n - F_{hd})\cos(\alpha) - M_S \ddot{x}''_n - M_p \ddot{x}''_n = 0 \tag{7}$$

$$(F_B + R_n - F_{hd})\sin(\alpha) - M_S \ddot{z}''_n = 0 \tag{8}$$

where M_p is the mass of a single piston, and A_p is the pressured area. The friction inside the piston bore is ignored in the analysis because the friction is very small comparing to the pressure force when pumping pistons are well lubricated.

Since M_S is the mass of a single slipper, the position of the coordinate system $x'' - y'' - z''$ related to the $x - y - z$ can be determined as:

$$x''_n = x_n + X_S \cos(\alpha) \tag{9}$$

$$z''_n = z_n + X_S \sin(\alpha) \tag{10}$$

Combining Eqs. (6), (7), (8), (9) and (10) yields:

$$\begin{aligned} &-[M_S X_S \sin(\alpha) + (M_p + M_S)\sec(\alpha) r_s]\ddot{x}_n \\ &+ M_S X_S^2[\cos(\alpha)\dot{\alpha}^2 + \sin(\alpha)\ddot{\alpha}]\sin(\alpha) \\ &+ M_S X_S[\ddot{z}_n + X_S\sin(\alpha)\dot{\alpha}^2 - X_S\cos(\alpha)\ddot{\alpha}]\cos(\alpha) \\ &+ F_{hd} r_h + (\{A_p P_n + M_S[X_S\cos(\alpha)\dot{\alpha}^2 \\ &+ X_S\sin(\alpha)\ddot{\alpha}]\}\sec(\alpha) - F_B + F_{hd}) r_s - I_{yy}\ddot{\alpha} = 0 \end{aligned} \tag{11}$$

The rotating trajectory of a piston assembly about the shaft axis is shown in Figure 1. The displacement of the piston along the x-axis is (Manring, 1999):

$$x_n = r\tan(\alpha)\sin(\theta_n) + a\sec(\alpha) + e\tan(\alpha) \tag{12}$$

The instantaneous acceleration of the piston assembly in the x-axis may be yielded by differentiating Eq. 12 twice with respect to time, such that

$$\ddot{x}_{\rm n} = \left(\frac{r\ddot{\alpha}}{\cos^2(\alpha)} + \frac{2r\dot{\alpha}^2\sin(\alpha)}{\cos^3(\alpha)} - r\tan(\alpha)\dot{\theta}_{\rm n}^2\right)\cdot\sin(\theta_{\rm n}) + \frac{2r\dot{\alpha}\dot{\theta}_{\rm n}}{\cos^2(\alpha)}\cos(\theta_{\rm n}) + \left(\frac{\ddot{\alpha}+2\dot{\alpha}^2\tan(\alpha)}{\cos^2(\alpha)}\right)e \tag{13}$$

where $\ddot{\theta}_{\rm n}$ can be ignored in the steady-state operating of the pump, and the offset $a = 0$ for most designs.

The displacement of a piston assembly along the z-axis direction is:

$$z_{\rm n} = r\sin(\theta_{\rm n}) + e \tag{14}$$

Similarly, the instantaneous acceleration can be derived as:

$$\ddot{z}_{\rm n} = -r\sin(\theta_{\rm n})\dot{\theta}_{\rm n}^2 \tag{15}$$

Since the swash plate usually travels in a small range and the most instability occurs in the event of high pressure standby or cutoff of the axial piston pump, the swash plate angle is closed to zero. Therefore, it is approximated that $\sin(\alpha) \approx \tan(\alpha) \approx \alpha$, $\cos(\alpha) \approx 1$, $(M_{\rm S}+M_{\rm p})r_{\rm s}\sec(\alpha) > > M_{\rm S}X_{\rm S}\sin(\alpha)$, $X_{\rm S} >> r_{\rm s}\tan(\alpha)$. Thus, substituting Eqs. 13 and 15 into Eq. 11 yields:

$$\begin{aligned}&[I''_{\rm yy} + (M_{\rm p}+M_{\rm S})(r\sin(\theta_{\rm n})+e) + M_{\rm S}X_{\rm S}^2]\ddot{\alpha}\\ &= M_{\rm S}r_{\rm s}X_{\rm S}\dot{\alpha}^2 - 2(M_{\rm p}+M_{\rm S})r_{\rm s}r\dot{\theta}_{\rm n}\cos(\theta_{\rm n})\dot{\alpha}\\ &\quad +(M_{\rm p}+M_{\rm S})rr_{\rm s}\dot{\theta}_{\rm n}^2\cdot\sin(\theta_{\rm n})\alpha\\ &\quad -M_{\rm S}X_{\rm S}[r\sin(\theta_{\rm n})\dot{\theta}_{\rm n}^2] + F_{\rm hd}r_{\rm h}\\ &\quad +(\{A_{\rm p}P_{\rm n}\} - F_{\rm B} + F_{\rm hd})r_{\rm s}\end{aligned} \tag{16}$$

in which the pressure balance force $F_{\rm B}$ is caused by the fluid film between the slipper pad and swash plate surface.

By using the first order Taylor expansion, the term of $\dot{\alpha}^2$ can be linearized in its desired conditions (α_0 and $\dot{\alpha}_0$) such that $\dot{\alpha}^2 = \dot{\alpha}_0^2 + 2\dot{\alpha}_0\ddot{\alpha}_0(\dot{\alpha} - \dot{\alpha}_0)$ Therefore, Eq. 16 can be written as:

$$\ddot{\alpha} = D(\theta_{\rm n})[B(\theta_{\rm n})\dot{\alpha} + C(\theta_{\rm n})\alpha + U(\theta_{\rm n})] \tag{17}$$

where

$$D(\theta_{\rm n}) = \frac{1}{I''_{\rm yy} + M_{\rm S}X_{\rm S}^2 + (M_{\rm p}+M_{\rm S})r_{\rm s}[r\sin(\theta_{\rm n})+e]},$$

$$B(\theta_{\rm n}) = 2r_{\rm s}[M_{\rm S}X_{\rm S}\dot{\alpha}_0\ddot{\alpha}_0 - (M_{\rm p}+M_{\rm S})r\dot{\theta}_{\rm n}\cos(\theta_{\rm n})],$$

$$C(\theta_{\rm n}) = (M_{\rm p}+M_{\rm S})rr_{\rm s}\dot{\theta}_{\rm n}^2\sin(\theta_{\rm n}),$$

$$U(\theta_{\rm n}) = M_{\rm S}X_{\rm S}r_{\rm s}\dot{\alpha}_0^2(1-2\ddot{\alpha}_0) - M_{\rm S}X_{\rm S}r\sin(\theta_{\rm n})\dot{\theta}_{\rm n}^2 + F_{\rm hd}(r_{\rm h}+r_{\rm s}) + (A_{\rm p}-\xi)r_{\rm s}P_{\rm n}$$

Then the dynamics of a piston assembly may be described by a linearized second order model by using Laplace transform, such that:

$$G(s) = \frac{D(\theta_{\rm n})}{s^2 - D(\theta_{\rm n})\cdot B(\theta_{\rm n})s - D(\theta_{\rm n})\cdot C(\theta_{\rm n})} \tag{18}$$

where s is a complex argument and $G(s) = \frac{\alpha(s)}{U(s)}$ is the transfer function, the coefficients of the transfer function vary periodically with piston angular positions and operating conditions of $\dot{\alpha}_0$ and $\ddot{\alpha}_0$.

The input to the linearized model is a lumped term including the constant input (such as $F_{\rm hd}(r_{\rm h}+r_{\rm s})$) and angular-varying inputs (i.e., $(A_{\rm p}-\xi)r_{\rm s}P_{\rm n}$ and $M_{\rm S}X_{\rm S}r\sin(\theta_{\rm n})\dot{\theta}_{\rm n}^2$). The term of $M_{\rm S}X_{\rm S}r_{\rm s}\dot{\alpha}_0^2(1-2\ddot{\alpha}_0)$ can be ignored because it is common to assume $\alpha_0, \dot{\alpha}_0 < < 1$ (Manring, 2001). The piston pressure of $P_{\rm n}$ changes from the discharge to intake pressure and vice versa in the pump that is determined by the valve plate timing from inlet to outlet ports. As the input to a second-order system, smoother transition $P_{\rm n}$ is preferred to ensure piston assemblies be able to follow the swash dynamics effectively. The sudden changes of $P_{\rm n}$ not only can cause the unstable tilting of the slipper, but generate the fluid borne high frequency noise.

Since there are no zeros in the numerator of the second-order model, the assemblies' dynamics are dominated by a pair of dominant poles determined by roots of the denominator. Therefore, the stability condition of the slipper and design robustness can be examined by dominant poles that are defined by some design parameters such as $M_{\rm p}$, $X_{\rm S}$, $I''_{\rm yy}$, etc. These factors can affect the response time, oscillations, damping ratio, and natural frequency of each piston assembly consequently. The coefficients $D(\theta_{\rm n})$, $B(\theta_{\rm n})$, and $C(\theta_{\rm n})$ are periodical functions of the shaft angle from 0 to 2π that alternates the poles periodically as well such that average poles between 0 and 2π (for the real and imaginary parts individually in the complex plane) can be calculated to indicate the stability and design robustness of parameters. If the location of average poles demonstrates a certain trend of poles movement caused by design parameter modifications, it can provide the evidence of dynamic characteristics and design recommendations. Otherwise, the random motions of poles are not able to direct the design.

3. Results and discussion

System poles of the transfer function Eq. 18 are calculated by the characteristic polynomial such that $\lambda^2 - D(\theta_{\rm n})\cdot B(\theta_{\rm n})\lambda - D(\theta_{\rm n})\cdot C(\theta_{\rm n})$, where λ is the Eigen values. There are a number of design parameters of the piston assembly that impact on $D(\theta_{\rm n})$, $B(\theta_{\rm n})$, and $C(\theta_{\rm n})$. To analyze the linearized model, a numerical example of the piston pump is presented, and the related parameters are listed in Table 1.

The pump rotates in a constant speed of 2200 rpm and has a maximum swash angle α_0 = 16 deg . During operating, signs of the tilting speed $\dot{\alpha}$ and acceleration $\ddot{\alpha}$ can be same or different. If $\dot{\alpha}\cdot\ddot{\alpha} < 0$, the stability conditions is able to use a Lyapunov function $V = \frac{1}{2}\dot{\alpha}^2$ to determine. Thus, the condition $\dot{V} = \dot{\alpha}\cdot\ddot{\alpha} < 0$ ensures the slipper asymptotically stable, which requires the input $U(\theta_n)$ to be satisfied with:

Table 1. Design parameters of piston assembly and pump.

Symbols	Descriptions	Value	Unit
e	Offset between the swash rotating center and the pump shaft axis x'	0.35	cm
M_P	Mass of one piston	0.18	kg
M_S	Mass of one piston slipper	0.07	kg
r_s	The supporting radius that is assumed as the average of the sealing and non-sealing lands on the slipper	1.3	cm
X_S	Distance between the slipper ball-joint center and its gravity center	0.98	cm
I''_{yy}	Moment inertia of the slipper about its gravity center around the $\bar{y}$ direction	5.1×10^{-6}	kg m^2
r	Pitch radius of the rotating group	4.6	cm

$$D(\theta_n)[B(\theta_n)\dot{\alpha}^2 + C(\theta_n)\alpha\dot{\alpha} + U(\theta_n)\dot{\alpha}] \le 0 \qquad (18)$$

In hydraulic engineering, this ideal condition means that the slippers will grind to a halt with the opposite tilting velocity and acceleration, and eventually reach its final resting state, which is called the attractor (i.e., α_0). However, the condition is too strict to always exist for the input signal that includes the pressure profile P_n. In this case, the stability condition of the slipper is only a concern while $\dot{\alpha} \cdot \ddot{\alpha} > 0$, in which both the tilting speed and acceleration increase and decrease at the same time. In the numerical example, the rise time of the pump flow from minimum to maximum is 90 ms, as the swash plate rotates from 0 to 16° and the rotating speed is about 3.2 rad/s. Generally, the axial piston pump is most vulnerable to approach the instability when the pump operates in the high-pressure standby mode, i.e. $\alpha \approx 0$. However, it can be assumed α_0 has any angular position to linearize the model of (18). The worst case (while the

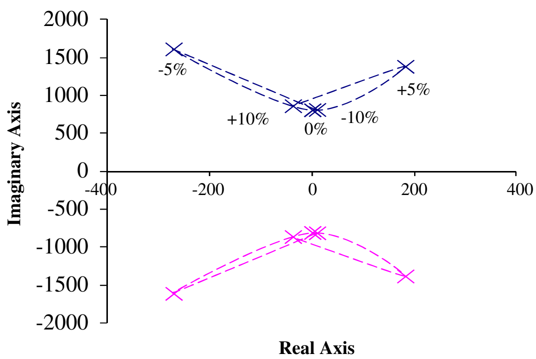

Figure 3. Poles movement by r.

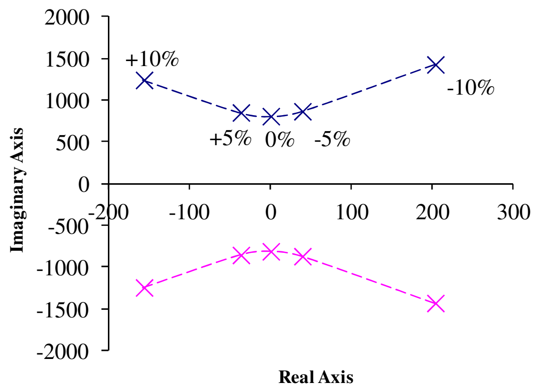

Figure 4. Poles movement by e.

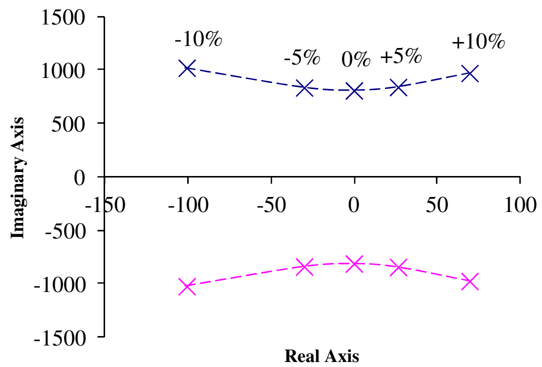

Figure 5. Poles movement by M_p.

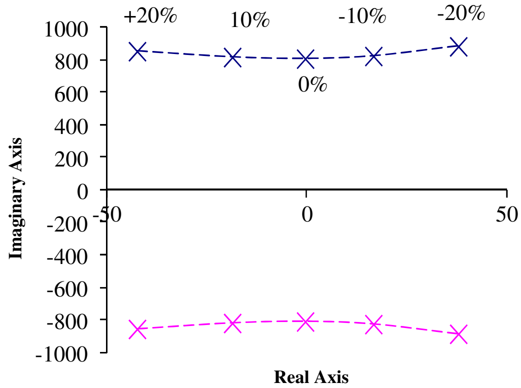

Figure 6. Poles movement by M_S.

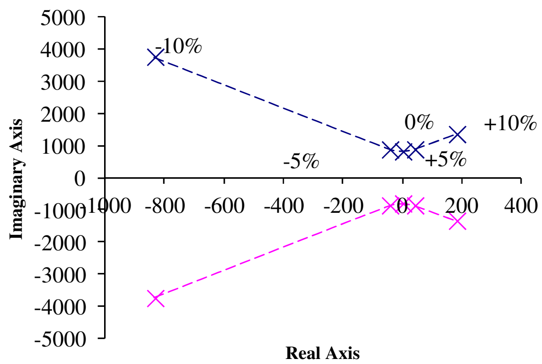

Figure 7. Poles movement by r_s.

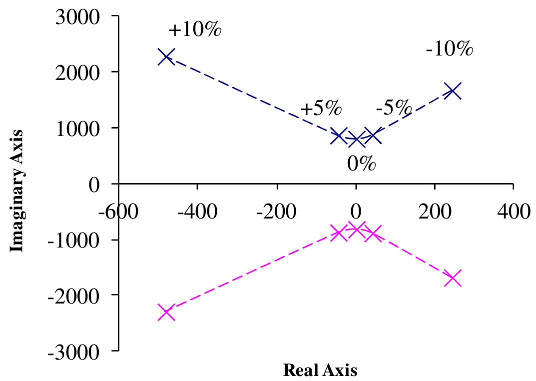

Figure 8. Poles movement by X_S.

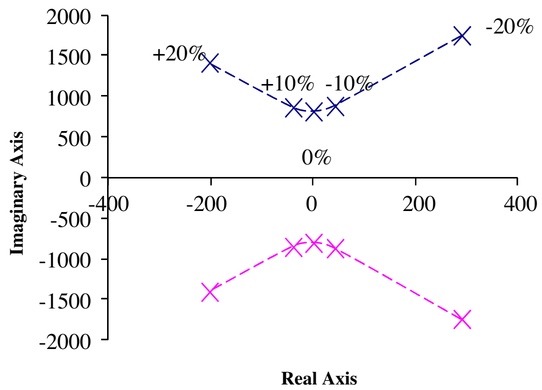

Figure 9. Poles movement by I''.

swash plate reach its maximum rotating acceleration 32 00rad/s^2) is used to analyze the stability condition. The sampling rate for acquisition is 1000Hz. To observe outcomes of driving the system poles by parameters, design parameters are tuned by ± 5%, ± 10%, ± 20% separately. Since these design parameters are sensitive to dynamic performance and precise manufactured in the piston pump, the modification of each design parameter is not available to make in practice and their impact on the pump performance can be varied.

For the dynamic system of (18), the real and imaginary parts of poles are averaged from 0 to 2π and visualized in the complex plane. As magnifying or minimizing the parameter pitch radius r even in a small range, the movement of poles is random and cannot show a certain move to the left or right as shown in Figure 3. It is difficult to conclude that tuning r may affect the dynamics of piston assemblies in a certain manner. However, in Figures 4–9, the parameters of e, M_P, M_S, r_s, X_S, and present the definite impacts on poles in this specific design. The larger parameters of e, M_S, X_s and I''_{yy} move the poles left and provide a more stable margin. On the contrary, smaller M_P and r_s make the system more stable in this special case because the reaction force R_n is assumed to de-stroke the slipper during operation. In the design case, M_S and are able to behave the certain

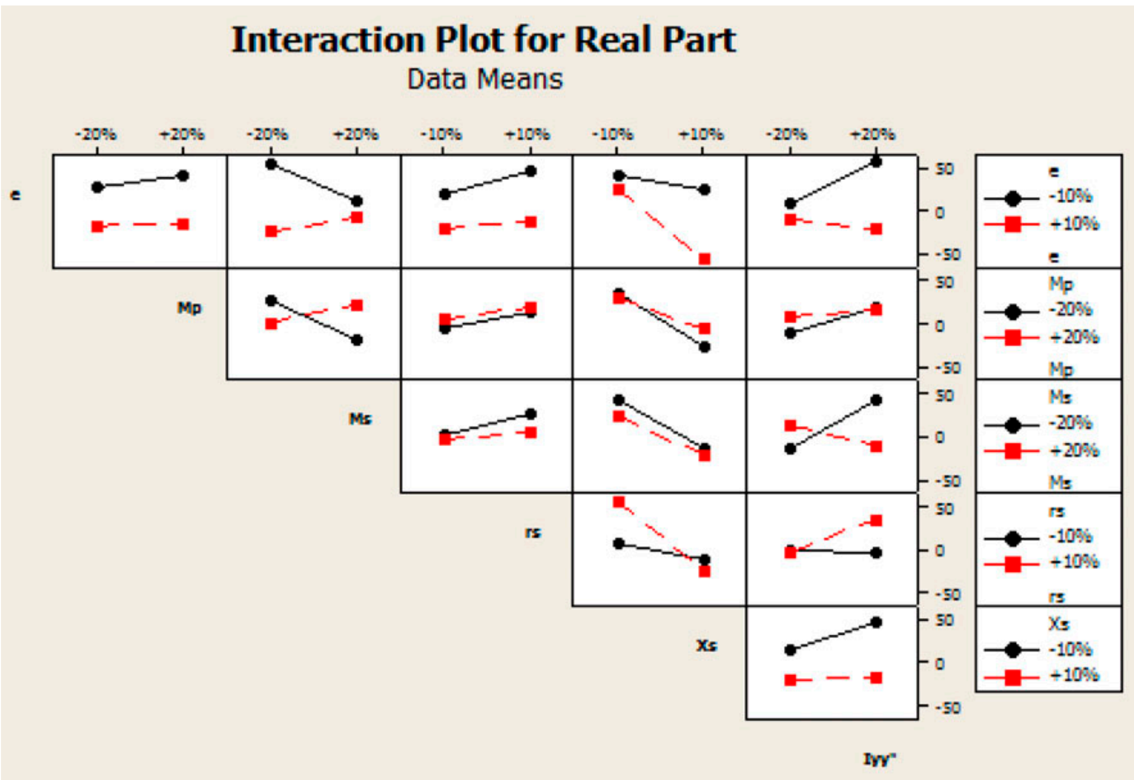

Figure 10. Interactions of the real part of poles by design parameters.

effects on the stability in a large tuning range ± 20%. Larger M_S will decrease the stability margin in the design because a large mass of slipper needs more modulating efforts to get it off steady-state. The total moment inertial of slipper I''_{yy} has the similar influence on the design robustness. e, M_P, r_s, and X_S, are more sensitive that only show the definite effect in a small tuning range of ± 10%. Otherwise, their impacts will be unascertainable similar to the pitch radius r. The mass of piston has opposite effects on the stability in comparison with the slipper mass because the M_P can offer more stabilized inertial to the whole assembly system. e, r_s and X_S are more case-based design parameter. In the case, the smaller offset e requires less control torque from swash plates that help stabilize the piston assembly. The supporting land radius of r_s can have the slipper less stable because of R_n. A large rotating arm of X_S help the slipper more stable in the case.

The above results are calculated by only tuning one parameter at a time and keeping the remaining parameters unchanged. In the PPA study, the effect of one factor depends on the level of other factors. The interactions of the parameters e, M_P, M_S, r_s, X_S, and I''_{yy} may affect the moving trends of poles in the complex plane. Figure 10 shows the mean values of the real part of poles in the interaction plot to illustrate possible interactions of parameters. Two levels of parameter tuning generate a matrix of interactions that present impacts by one parameter in different levels (± 10% or ± 20%) on the other parameter. Only e and M_P show parallel lines in the plot that means little impact on each other. Other parameters are associated with each other to influence the dynamic stability. The greater is the difference of two-line slopes in the plot, the higher degree of interaction the two design parameters have.

The simulation results based on the PPA method shown in Figures 3–9 present the effects of varying design parameters in the particular case. Since the hydraulic piston pump is a high precision machining equipment and operating condition based, the variations of some parameters may provide different effects in different design cases. The method proposed in the research can be used to direct the designers to find a straightforward clue to modify their designs based on the simulation and test results. The test validations can be proceeded base Design of Experiments (DOE) which has similar concept to PPA in the laboratory. The method in the research can be used to direct the DOE and PPA work and save much engineering trial and error efforts.

4. Conclusions

The movements of reciprocating, rotating about the shaft, and tilting toward the swash plate make the piston assembly have the most complicated dynamics and design difficulties in axial piston pumps. During the normal operating, the slippers have to effectively follow their desired dynamics, i.e. swash plate angle and velocity, otherwise tilting and lifting instability of piston assemblies may occur. The paper develops a second-order linearized model to analyze stability and robust design of piston assemblies. Poles movement of the model are dominated by design parameters of the piston assembly and rotating group such that the PPA approach is used to investigate their impacts on the assembly motions and ensure stability. Although the model has angular-varying system inputs and coefficients caused by the pump rotating and operating conditions, averaged poles are able to demonstrate the assembly's dynamics and stability margin. The impacts on stability margins of each parameter and interactions can be referred for the robust design of the rotating group and piston assemblies.

Nomenclature

A_p	Piston section area
a	Offset between the slipper ball joint and the surface of the swash plate
e	Offset between the swash plate pivot and the shaft center-line of the pump
F_{hd}	Hold-down force exerting on a single slipper
F^x_{Sn}, F^z_{Sn}	Reaction exerting on the slipper by the piston along the x, z axes
$\dot{H}''_n$	The time rate-of-change of angular momentum for a single slipper about its gravity center
I''_{yy}	Moment inertia of the slipper about its gravity center around the y-axis direction
$M^y_{hd}, M^y_{Sn}, M^y_n, M^y_B$	Moments about the gravity center of the slipper produced by the hold-down device, piston, swash plate and balance pressure individually
M_p	Mass of a single piston
M_S	Mass of a single slipper
n	Piston and slipper counter
P_n	Piston-bore pressure
R_n	Reaction on the nth slipper exerted by the swash plate
r	Piston pitch-radius
r_h, r_s	The inner radius of the slipper retainer and the slipper supporting radius
X_S	Distance between the slipper pivot center and its gravity center
$x, y, z, \dot{x}, \dot{y}, \dot{z}, \ddot{x}, \ddot{y}, \ddot{z}$	Displacements, velocities and accelerations of the piston along x, y, z axes directions individually
x_{Sn}, y_{Sn}, z_{Sn}	Positions of the exerting point of the piston reaction with respect to the gravity center of the slipper along x, y, z axes
x - y - z	Cartesian coordinates with a origin on swash rotating center
x' - y' - z'	Cartesian coordinates with a origin on the shaft center-line

$x'' - y'' - z''$ Cartesian coordinates with a origin on the slipper gravity center
α, $\dot{\alpha}$, $\ddot{\alpha}$ Slipper tilt angle, velocity and acceleration
α_0, $\dot{\alpha}_0$, $\ddot{\alpha}_0$ Swash plate angular displacement, velocity and acceleration
θ_n, $\dot{\theta}_n$, $\ddot{\theta}_n$ Angular position, velocity and acceleration of the rotating kit

Notes on contributor

Shu Wang received his B.S. and M.S. in mechanical engineering, respectively, in 1994 and 1997. He had worked as a mechanical engineer in the aircraft industry for a number of years. In 2003, he joined the fluid power group at University of Saskatchewan and received his Ph.D. degree in 2007. He was a scholarship student at the University of Saskatchewan, and researched and taught classes in Mechanical Engineering Design. He is currently a lead engineer in Eaton Corporation in Eden Prairie, Minnesota. His research interests mainly lie in mechatronics, dynamic control systems, hydraulic control systems, and on-line state/parameter estimation.

References

Ahn, S. Y., Rhim, Y. C., and Hong, Y. S. 2005. Lubrication and dynamic characteristics of a cylinder block in an axial piston pump. *Proceedings of the World Tribology Congress III – 2005*, Washington, D.C., pp. 223–224.

Alyaqout, S. F., Papalambros, P. Y., and Ulsoy, A. G. 2010. Combined Robust Design and Robust Control of an Electric DC Motor. *IEEE/ASME Transactions on Mechantronics*, Vol. 99, pp. 1–9.

Du, H. 2002. Pressure Control with Power Limitation for Hydraulic Variable Displacement Piston Pumps. *Proceedings of the 2002 American Control Conference*, Vol. 2, pp. 940–945.

Greenwood, D. T. 1988. *Principles of Dynamics*, Prentice-Hall Inc., New Jersey.

Harris, R. M., Edge, K. A., and Tilley, D. G. 1996. Predicting the Behavior of Slipper Pads in Swash Plate-Type Axial Piston Pumps. *ASME Journal of Dynamic Systems, Measurement and Control*, Vol. 118, No. 1, pp. 41–47.

Iboshi, N., and Yamaguchi, A. 1982. Characteristics of a Slipper Bearing for Swash Plate Type Axial Piston Pumps and Motors – 1: Theoretical Analysis. *Bulletin of the JSME*, Vol. 25, No. 210, pp. 1921–1930.

Iboshi, N., and Yamaguchi, A. 1983. Characteristics of a Slipper Bearing for Swash Plate Type Axial Piston Pumps and Motors. *Bulletin of the JSME*, Vol. 26, No. 219, pp. 1583–1589.

Lin, T. Y., and Yak, A. S. 2000. Reliability by robust design for optical alignment in a CD pickup. *IEEE/ASME Transactions on Mechantronics*, Vol. 5, No. 4, pp. 386–393.

Manring, N. 1999. The Control and Containment Forces on the Swash Plate of an Axial-Piston Pump. *ASME Journal of Dynamic Systems, Measurement, and Control*, Vol. 121, pp. 599–605.

Manring, N. 2001. The Control Torque on the Swash Plate of an Axial-Piston Pump Utilizing Piston-Bore Springs. *ASME Journal of Dynamic Systems, Measurement, and Control*, Vol. 121, pp. 599–605.

Manring, N. D. 2002. The Control and Containment Forces on the Swash Plate of an Axial Piston Pump Utilizing a Secondary Swash-Plate Angle. *Proceedings of the American Control Conference*, Anchorage, AK, pp. 4837–4842.

Manring, N. D., and Johnson, R. E. 1996. Modeling and Designing a Variable-Displacement Open-Loop Pump. *ASME Journal of Dynamic Systems, Measurement, and Control*, Vol. 118, pp. 267–271.

Manring, N., Johnson, R. E., and Cherukuri, H. P. 2002. The Impact of Linear Deformations on Stationary Hydrostatic Thrust Bearings. *ASME Journal of Tribology*, Vol. 124, pp. 874–877.

Manring, N., Wray, C. L., and Dong, Z. 2004. Experimental Studies on the Performance of Slipper Bearing within Axial-Piston Pumps. *ASME Journal of Tribology*, Vol. 126, pp. 511–518.

Merritt, H. E. 1967. *Hydraulic Control Systems*, John Wiley, New York.

Schoenau, G. J., Burton, R. T., and Kavanagh, G. P. 1990. Dynamic Analysis of a Variable Displacement Pump. *ASME Journal of Dynamic Systems, Measurement, and Control*, Vol. 112, pp. 122–132.

Yamaguchi, A. 1976. Motion of Pistons in Piston-Type Hydraulic Machines – 3 Exponential Function-Type Piston. *Bulletin of the JSME*, Vol. 19, No. 130, pp. 413–419.

Zeiger, G., and Akers, A. 1985. Torque on the Swashplate of an Axial Piston Pump. *ASME Journal of Dynamic Systems, Measurement, and Control*, Vol. 107, pp. 220–226.

Zhang, X., Cho, J., Nair, S. S., and Manring, N. D. 2001. New Swash Plate Damping Model for Hydraulic Axial-Piston Pump. *ASME Journal of Dynamic Systems, Measurement, and Control*, Vol. 123, pp. 463–470.